Modeling of particle wet milling in a stirred tank using CFD/PBE coupled approach

Zoé Mercier, Pascal Fede, Maxime Pigou, Jean-Philippe Bayle, Eric Climent

MODELLING OF PARTICLE WET MILLING IN A STIRRED TANK USING CFD/PBE COUPLED APPROACH

Z. Mercier,[1,2,*] P. Fede,[1] M. Pigou,[1] JPh. Bayle,[2] & E. Climent[1]

[1]*Institut de Mécanique des Fluides de Toulouse (IMFT), Université de Toulouse, CNRS, Toulouse, France*

[2]*CEA, DES, ISEC, DMRC, Université de Montpellier, Marcoule, France*

*Address all correspondence to: Z. Mercier, E-mail: zoe.mercier@imft.fr

Original Manuscript Submitted: 01/13/2023; Final Draft Received: mm/dd/yyyy

Many industrial processes involve grinding and milling operations to produce powders of well-controlled particle size distribution. Improving these process requires to consider particle-particle interactions, breakage, aggregation, and in the case of wet milling, hydrodynamics. The goal of this study is to develop a numerical model, accounting for these mechanisms, with the final aim to guide the conception of an optimal process. A new method to solve particle size distribution inside a stirred tank is proposed. Computing fluid dynamics is coupled with a population balance model. The hydrodynamics of the multi-phase flow is solved using the mutli-fluid Euler approach, whereas the class method is considered to resolved the population balance equation. A theoretical definition of the breakage functions, based on hydrodynamics inside the tank, is proposed. Preliminary results show that breakage is highly heterogeneous inside the tank and that particle breakage frequency allow to evaluate mill efficiency.

KEY WORDS: *wet milling, computing fluid dynamics, population balance model, stirred tank*

1. INTRODUCTION

Milling process is a common operation unit in many industries such as pharmaceutical, food, paint and nuclear. Different designs of mill exist, they can either be oriented horizontally or vertically, be composed of a stirred or not, and work in dry or wet conditions. However, wet milling appears to be an interesting alternative to usual dry milling in terms of time and energy saving. A vertical wet milling composed of a stirred and grinding media is considered here. The study of such process is currently ongoing since its improvement can lead to higher production rate and better quality of the resulting powder. The modelling and numerical simulation of this process is challenging due to the large variety of time and length scales interacting with each other. Indeed, on one hand the macro-scale (mill scale hence about 10 to 100 centimeters) provides information on the flow main hydrodynamics; on the other hand, the micro-scale (particles of few microns) describes mechanisms sustained by the particles as breakage and/or aggregation. Phenomenological methods are the most widely used models to predict efficiency of milling and influence of operating parameters (Bilgili and Guner, 2021). The stressing energy model proposed by Kwade (1999a) defines the stressing energy and stressing frequency as functions of

0276–1459/18/$35.00

operating parameters (such as bead diameter, bead density, stirred rotation and volumetric fraction). The stressing energy describes the upper limit of the energy transferred from the stirred to the bead. On the other hand stressing frequency estimates the number of times a particle is stressed between beads within a specified time. Hence, stressing frequency is proportional to the collision frequency of grinding media, and higher values of stressing frequency are beneficial for the milling process. This method has the advantage to be quickly applicable, however it over-predicts the mean stress energy and the mean frequency of contact by several orders of magnitude (Beinert et al., 2014). Moreover, it does not predict the particle size distribution. In order to overcome those drawbacks, mechanistic modelling approaches are used. Mechanistic models incorporate some hydrodynamic considerations into breakage mechanism. In a stirred mill, because particles are orders of magnitude smaller than grinding media, the particle suspension is treated as a single equivalent flow with a Newtonian behaviour, whereas grinding medias constitute a dispersed solid phase (Bilgili and Guner, 2021). Most of the time Euler-Euler or Euler-Lagrange approaches are used for multi-phase flow simulation. The most popular approach in the modeling of wet stirred media milling is the CFD-DEM Euler-Lagrange based approach, which tracks all the beads and treat explicitly collisions (Bilgili and Guner, 2021). However, this approach has computational tractability limitations and can hardly be applied at industrial scale. For their better tractability, Euler-Euler approaches are therefore better suited for industrial contexts. All the studies done on two-phase flow in stirred media mill aim to develop an understanding of the hydrodynamics, and beads motion inside the mill. However, they do not predict the evolution of particle size distribution, for which a Population Balance Model (PBM) can be used. The Population Balance Equation (PBE) describes the particle size distribution over time. Breakage kernel is needed in the source term of this equation. Most of the time breakage kernel (or breakage rate) is defined by experimental investigations (Bilgili and Scarlett, 2005; Capece et al., 2011). However, the experimental breakage kernel is only meaningfull for the operating parameters considered and is not extendable to other operating parameters. Hence, this experimental kernel could not be used for predicting the influence of operating parameters. Nomura et al. (1991a) proposed a theoretical approach where the breakage kernel is expressed in terms of operational conditions and the nature of considered materials. Recently, Oliveira et al. (2020) proposed a model based on DEM simulations, to simulate breakage in dry milling. However, as mention in the paper, under wet milling the simulations do not account for the fluid. Moreover, for both studies mentioned above, a perfectly mixed mill is assumed. To the best of the authors knowledge, there is no study taking into account particle transport into the mill.
The present work proposes new numerical methods. The multiphase flow is solved using a generalized multi-fluid Euler method (Fede et al., 2016), which means that equivalent fluid assumption is not necessary. Particles motion is solved. In addition, the breakage kernel is theoretically defined and depends on local properties of the hydrodynamic. The following section gives an an overview of the numerical methods for modeling a multiphase flow in a stirred tank, then population balance model is introduced. Thereafter model of breakage functions is described, before giving details of two different coupled methods. Finally, preliminary simulation results are exposed.

2. NUMERICAL MODEL OF MULTI-PHASE FLOW IN A STIRRED TANK

The system investigated in this study consists of a cylindrical tank agitated by a boat propeller (figure 1). The height of the tank is about 80mm and the diameter is 66mm. The grinding beads and the particles are both considered as spherical. Volume ratio between grinding medias and

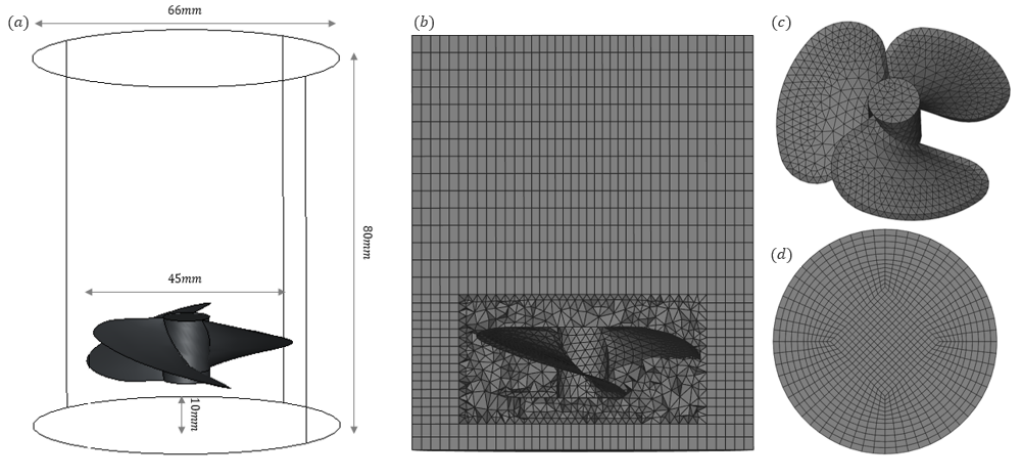

FIG. 1: Geometry (a) and Mesh of the stirred tank (front view (b), propeller (c), top view (d))

particles to mill is on the order of 10^6, whereas the density ratio is around 0.5. The propeller velocity is $600rpm$. In numerical simulations, the rotating motion of the propeller is taken into account by solving the equations governing the fluid in a rotating frame. The centrifugal and Coriolis accelerations are added to the momentum equations. This method is feasible because no fixed elements are inside the tank (as counter-blades, extraction pipes, ...). Otherwise, a Multiple Frames of Reference approach like that described by Bennani et al. (2017) should be used.

Figure 1 shows the mesh of the tank and the propeller. O-grid technique has been used to construct the mesh in order to have nearly uniform cells. However, because of the shape of the boat propeller, tetrahedral cells are used near the blade. The mesh contains 88 000 cells. Validity of the mesh have been studied by comparing the power supplied and the power dissipated in a single-phase flow. This power ratio is known as the power number. An accurate mesh should be able to predict it (Deglon and Meyer, 2006). For high Reynolds number, the power number only depends on propeller geometry (Roustan et al., 1999). The Reynolds number, defined as $R_e = \omega D^2 \rho_f / \mu$, is order of 10^6 where ω, D, ρ_f and μ are respectively the angular velocity, the propeller diameter, the fluid density and the dynamic viscosity. The power supplied is given as $P_s = \rho_f \left(\omega/2\pi\right)^3 D^5$. The power dissipated P_d can be expressed in term of the dissipation of kinetic turbulent energy ε as $P_d^{\varepsilon} = \int_\Omega \rho_f \varepsilon$. This power can also be seen as a function of the torque applied on the blade τ as $P_d^{\tau} = \omega\tau$. The power number obtained numerically with both of those methods are respectively 0.25 and 0.41. Those values are close to the experimental one (which is 0.40), ensuring the good representation of the hydrodynamics inside the tank.

The flow inside the tank is a multi phase flow composed of a carrying fluid, grinding media (also named beads) and particles to mill. The multi-phase flow model used in this study is based on the multi-fluid Euler approach (Fede et al., 2016). Each phase is treated as a continuous and separated transport equations are solved for each phase coupled through inter-phase transfer terms. The fluid turbulence is modelled by using the $k - \varepsilon$ with additional terms taking into account the effect of the particle on the turbulence. For the solid phase (beads and particles) the kinetic theory of granular flow is used with a transport equation for the random particle kinetic energy q^2.

The numerical simulations presented in this paper have been carried out using neptune_cfd.

neptune_cfd is a multiphase flow software developed in the framework of the NEPTUNE project, financially supported by CEA, EDF, IRSN and Framatome (Neau et al., 2020).

3. POPULATION BALANCE MODEL

3.1 Population balance equation

In order to predict the particle size distribution, a population balance model is used. Over a population of particles, one can consider the number density function $f(\mathbf{c}_p, \xi; \mathbf{x}, t)$ as $f(\mathbf{c}_p, \xi; \mathbf{x}, t)d\mathbf{c}_p d\xi d\mathbf{x}$ is the probable number of particles with a velocity in $[\mathbf{c}_p; \mathbf{c}_p + d\mathbf{c}_p]$, with a volume in $[\xi; \xi + d\xi]$ and a center of mass located in $[\mathbf{x}; \mathbf{x} + d\mathbf{x}]$ at time t (Shiea et al., 2020).

From this probability density function, discretized number distribution function is defined. The continuous size distribution of volume is approximated by a finite number of class (Kumar et al., 2008; Kumar and Ramkrishna, 1996). For example, the k^{th} classes is represented by a volume υ_k, and upper and lower intervals $[\upsilon_{k-1/2}, \upsilon_{k+1/2}]$. Hence, the number distribution function can be defined as:

$$n_k(\mathbf{x}, t) = \int_{-\infty}^{\infty} \int_{\upsilon_{k-1/2}}^{\upsilon_{k+1/2}} f(\mathbf{c}_p, \xi; \mathbf{x}, t) d\xi d\mathbf{c_p} \tag{1}$$

$n_k(\mathbf{x}, t)d\mathbf{x}$ defines the probable number of particles whose volume lies in $[\upsilon_{k-1/2}, \upsilon_{k+1/2}]$ interval with a center of mass located in $[\mathbf{x}; \mathbf{x} + d\mathbf{x}]$ at time t. $k = 0$ refers to smaller particle, whereas $k = N$ is for the largest one.
The discretized population balance equation for breakage is given as :

$$\frac{\partial n_k}{\partial t} + \frac{\partial u_{k-,i} n_k}{\partial x_i} = \sum_{q=k}^{N} n_q \Omega_n f_b^c f_R f_C \beta_{qk} - n_k \Omega_n f_b^c f_R f_C \ . \tag{2}$$

The breakage operates a transfer of particles from the largest classes to the smaller ones. This is accounted for through the two terms on the right-hand side of (2). The first is refered to as the "birth term" and accounts for the breakage of larger particles which produces particles in the k^{th} class. The second term is the "death term" and accounts for the breakage of particles of this v_k into smaller particles. Note that for the model to be conservative, total volume rates of death and birth terms over all classes must cancel out.

3.2 Theoretical breakage functions

The birth term can be decomposed in three terms:

- $n_k \Omega_n$ is the number of particle available for the breakage. The possible nipping volume Ω_n is a corrected term which model the fact that not all particles are available.
- $f_b^c f_R f_C$ is the breakage kernel (also known as selection function S). It is the frequency to which particles are break.
- Finally β_{qk} is the discretized form of the β function which is the fragmentation distribution function. Basically, $\beta(\upsilon, \upsilon')$ is the number density of υ'-volume particle created by the breakage of a υ-volume particle.

The breakage kernel depends on operating parameters. In the literature, most of the time, this function is determined by experimental investigations. The aim of this paragraph is to obtain from theoretical considerations the breakage kernel in a stirred tank. The breakage kernel defines the probable number of particles having a given volume ground per unit of time. Various mechanisms responsible for breakage could be considered: shear of the flow, inter-particle collisions, bead-bead collisions or bead-wall collisions however following Kwade (1999b) the bead-bead collisions is the dominant mechanism. For having particle breakage controlled by inter-bead collisions three simultaneous conditions have to be achieved (Nomura et al., 1991b). First, the inter-bead collisions frequency has to be high. Second, the presence of the powder: particles should be between the colliding beads and should not be drained by the fluid during beads approaching movement. Finally the available energy for breakage given by the beads must be high enough to break particle. Hence, f_b^c is the mean inter-beads collisions frequency, f_R the rupture function and f_C the crushing one. The breakage kernel is the product of those three terms.

Bead collision frequency

The collision frequency is given as :

$$f_b^c = g_0 n_b^2 d_b^2 \pi \langle u_b^r \rangle \tag{3}$$

where $g_0 = \left(1 - \alpha_b/\alpha_{max}\right)^{-2{,}5\alpha_{max}}$ (Lun and Savage, 1986) is the radial distribution function which models the rise of collision frequency in dense flow ($\alpha_{max} = 0.64$ is the maximum random packing of spheres), n_b the number of grinding media per unit of volume $\alpha_b \rho_b = m_b n_b$ (where α_b, ρ_b and m_b are the volume fraction, the density and the mass of grinding beads), d_b is the grinding beads diameter, and $\langle u_b^r \rangle$ the mean relative velocity between grinding beads. Neglecting the correlation induced by the turbulence (Fede et al., 2015; Laviéville et al., 1997), this velocity is given by

$$\langle u_b^r \rangle = \sqrt{\frac{16}{\pi}\frac{2}{3} q_b^2}. \tag{4}$$

Crushing function

When particles are in the possible nipping volume, it does not necessarily mean that those particles are going to be nipped and crushed. Indeed, when two beads approach, particles can be ejected (Gers et al., 2010). Two colliding beads can capture a particle of size d_p if the particle enters in the possible nipping volume (see zone ABCD in figure 2) and stays without being ejected until the bead-bead distance is equal to particle size d_p. The crushing function model this two processes of entering and staying in the crushing zone. Hence the function is defined as the probability of entering between the two beads (zone ABCD) times the probability of not being ejected. Particles in the region EDFC are assumed to be nipped. Particles can enter the ABCD zone when the distance between the beads is greater than the particle size d_p. The probability of entering this zone is assumed to be equal to the ratio between the time period for the approaching bead to maintain the distance greater than d_p (Δt_e) and the time period for the bead to collide ($\tau_b^c = n_b/f_b^c$). $\Delta t_e = (\lambda - d_p)/u_b^r$ and $\tau_b^c = \lambda/u_b^r$. Hence $\Delta t_e/\tau_b^c = (1 - d_p/\lambda)$. The probability for a particle in the nipping zone not to be ejected is defined as the volumetric ratio of CDEF to ABCD zone. The volume of the CDEF zone is given by a cylinder of diameter d_b and height d_p. The volume of ABCD is the possible nipping volume Ω_n defined previously. Hence the probability of staying is equal to the ratio d_p over λ. Finally, the crushing function is defined

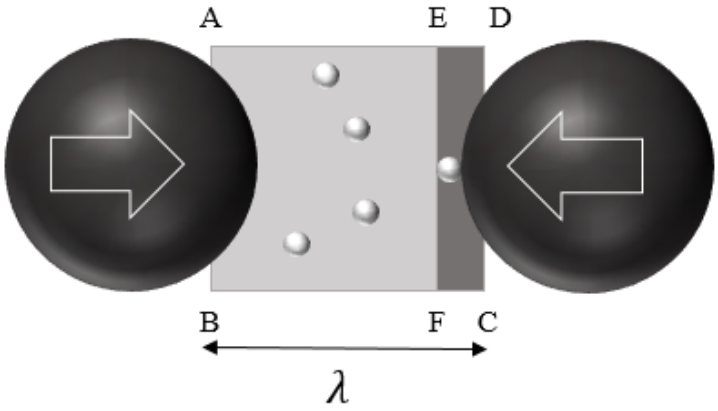

FIG. 2: Effective volume between two grinding media

as:

$$f_C = \frac{d_p}{\lambda}\left(1 - \frac{d_p}{\lambda}\right) . \tag{5}$$

Rupture function

Consider a particle of size d_p nipped by the bead. This particle could break only if the energy given by the bead is high enough. Rupture function defines this rupture condition as

$$f_R = 1 - exp\left(ln(0.5)\frac{E_b}{E_r}\right) \tag{6}$$

Where E_r is the energy required to break a particle. E_b is the energy given to the particles by the colliding beads $E_b = 1/2 m_b \langle u_b^r \rangle^2$.

Possible nipping volume

All particles inside a cell of size Ω are not captured during a collision between two beads. The zone of possible nipping is assumed to be a cylinder existing between two beads having a mean distance between each other of λ (figure 2). This volume, called the possible nipping volume Ω_n is hence defined as:

$$\Omega_n = \pi \left(\frac{d_b}{2}\right)^2 \lambda \tag{7}$$

where λ is the mean bead-bead distance and is written in terms of the collision frequency and relative velocity:

$$\lambda = \langle u_b^r \rangle \times \tau_b^c . \tag{8}$$

3.3 Fragmentation distribution function

Breakage can result in the formation of new particle whose size do not match with any representative sizes. In order to represented this particle, the fixed pivot method is used to discretize the

β function (Kumar and Ramkrishna, 1996). Hence,

$$\begin{aligned} \beta_{qk} &= \int_{\upsilon_{k-1}}^{\upsilon_k} b(\xi,\upsilon_k)\beta(\upsilon_q,\xi)d\xi \\ &+ \int_{\upsilon_k}^{\upsilon_{k+1}} a(\xi,\upsilon_k)\beta(\upsilon_q,\xi)d\xi \end{aligned} \tag{9}$$

Where,

$$a(\xi,\upsilon_k) = \frac{\upsilon_{k+1}-\xi}{\upsilon_{k+1}-\upsilon_k} \tag{10}$$

$$b(\xi,\upsilon_k) = \frac{\xi-\upsilon_{k-1}}{\upsilon_k-\upsilon_{k-1}} \tag{11}$$

a and b fractions are chosen in order to conserve the particle count and volume :

$$a(\xi,\upsilon_k) + b(\xi,\upsilon_{k+1}) = 1 \tag{12}$$

$$a(\xi,\upsilon_k)\upsilon_k + b(\xi,\upsilon_{k+1})\upsilon_{k+1} = \xi \tag{13}$$

Hence the volume is conserved $\sum_{i=0}^{j} \beta_{qk}\upsilon_k = \upsilon_q$.

4. COUPLED METHOD

The previous section, underlines that hydrodynamic information are needed to model breakage mechanisms. Hence a coupled CFD/PBE approach should be used to estimate particle size distribution. Two different coupled methods could be considered.

The first method considers each particle classes as a granular phase. The particle granular phases are represented by the mean volume of the class. Hence, N+2 phases are considered by this method: the fluid phase, the grinding media granular phase and the N particle granular phases. In order to account for the breakage, PBE right-hand side term of (2) is used to model an inter-phase mass transfer in the (N+2)-Phase Euler-Euler coupling.

An alternative method is to decrease the number of granular phases for the particles. Only one particle granular phase is considered and the amount of particles associated to each class is represented by passive scalars transported by this phase. To account for inter-phase momentum transfers between the 3 considered phases (liquid, beads, particles), the Euler-Euler model needs the mean particle diameter which, in this case, is deduced from the evolution of local Particle Size Distributions. The advantage of this method is to reduce computation time, indeed for the direct method $6 \times N$ partial differential equations are solved for the particle granular phases, whereas $6 + N$ partial differential equations are solved for the granular phases in the case of the second method. However, more assumptions are done in the one particle granular flow. As a matter of fact, it is assumed that all particles are transported at the same velocity, no matter their size. Hence, high local concentration of a class of particle (due to their sizes) can be hidden by this method.

5. RESULTS AND DISCUSSION

5.1 Predominant beads agitation mechanism

Breakage kernel is function of bead relative collision velocity. However several mechanisms could be the cause of this relative velocity, the aim of this section is to determine the predominant

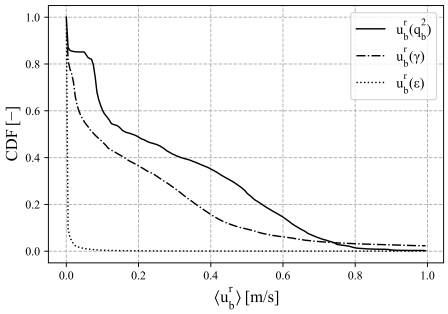

FIG. 3: Relative collision velocity measured in numerical simulation. The velocity is expressed in terms of the bead agitation for the full line, shear flow for the dashed line and dissipation turbulent kinetic energy for the dotted line.

mechanism.

- In the case where beads have non correlated velocities, the molecular chaos assumption can be applied. Hence, the relative collisions velocity is given by Eq. (4).
- The local shear flow γ could be an other mechanism leading to relative collision velocity between bead. In this case,
$$\langle u_b^r \rangle = d_b |\gamma| \, . \tag{14}$$
The local shear of the flow is given as $\gamma = \sqrt{\varsigma_{ij}\varsigma_{ij}}$, where ς is the velocity gradient.
- For small beads Stokes number, Saffman and Turner (1956) links the relative velocity of the beads with dissipation turbulent kinetic energy as:
$$\langle u_b^r \rangle = d_b \sqrt{\frac{2\varepsilon}{15\pi\nu}} \tag{15}$$

Figure 3 shows the cumulative distribution function (CDF) of the relative collision velocity for each mechanism measured in the whole stirred tank. We observed that the relative collision velocity expressed as a function of the bead agitation is higher in most of the tank. Local shear flow is responsible of high relative velocity but only for a small volume inside the tank. High velocity gradient near the wall or near the blade can be responsible for such value. Nevertheless, for the following studies, the relative collision velocity will be expressed in terms of bead agitation.

5.2 Coupled CFD/PBE results

Coupled CFD/PBE numerical simulations have been carried out using the one particle granular phase method with 10 classes. Here some preliminary results were presented. Binary symmetric breakage is considered, which means that a mother particle break in two equal volume particles. Initial particle size is about ten microns. Figure 4 shows local distribution of bead volume fraction (a) and bead kinetic energy (b). The first observation is that beads are more concentrated above and under the propeller. However those beads are less agitated. Indeed bead kinetic energy is much larger near the blades of the propeller. Particle volume fraction is heterogeneous inside the tank (see figure 5). Particles are more concentrated at the bottom of the tank.

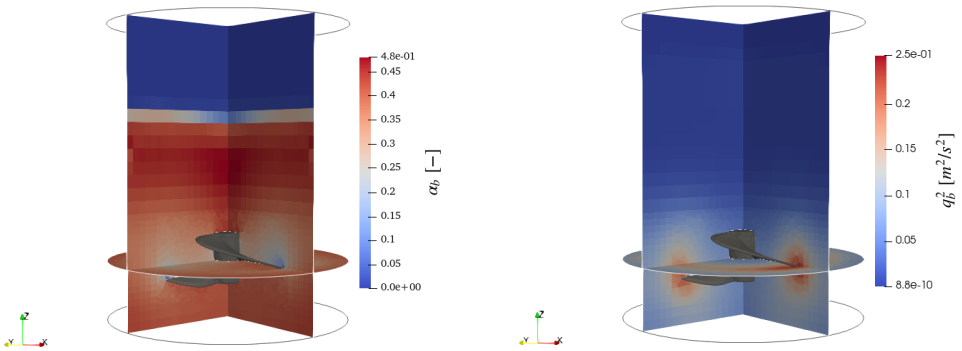

(a) (b)

FIG. 4: Local distribution of bead volume fraction (a) and bead kinetic energy (b).

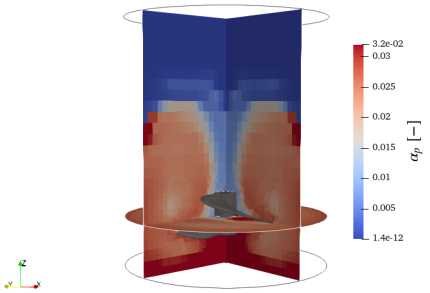

FIG. 5: Local distribution of particle volume fraction

Profile along z axis (at different radius r) of the volume fraction of bead and particle are presented on figure 6. Grey lines give bottom and top positions of the boat propeller. It is shown, that there is stratification effect on the bead inside the tank. Indeed the volume fraction of bead is higher above the propeller. Regarding particle, they are much concentrated on the lower part of the tank.

Relative collision velocity is largest near the propeller (see figure 7 (a)). Beyond 0.035m, the velocity is close to zero, even if a significant amount of beads are there. Collision frequency, which is function of relative collision velocity and volume fraction is represented on figure 7 (b). On a same x-axis, collision frequency increases when the distance to the bottom of the tank decreases. Indeed, the largest values of collision frequency are bellow the propeller. The crushing function has the same profiles as bead volume fraction, hence particle are more likely to be nipped and crushed near the propeller or close to the wall. Breakage is not limited by the energy given by the beads. Indeed, rupture function is equal to one. To sum up, breakage kernel seems to be higher in the lower part of the tank. This coincide with particle volume fraction, meaning that breakage will be efficient. However, above the propeller, collision frequency decreases, suggesting that particle will less break. To estimate the breakage efficiency the effective particle volume (volume of particle inside the possible nipping zone) times the breakage kernel can be considered (see figure 8). This quantity corresponds to the volume of particle break per unit time. Particles are more subject to breakage at the bottom of the tank than above the propeller. As a matter of

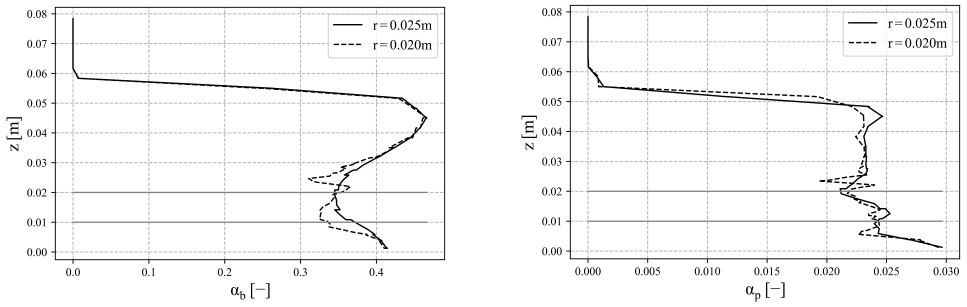

(a) (b)

FIG. 6: z - profile of (a) bead volume fraction and (b) particle volume fraction.

fact, as we saw, particle volume fraction and bead collision frequency are larger at this place. Accordingly, particle mean diameter is smaller at the bottom of the tank (figure 8 (b)). In the wake of the propeller, breakage efficiency decrease.

Figure 9 presents particle breakage frequency and mean diameter profiles along x axis bellow

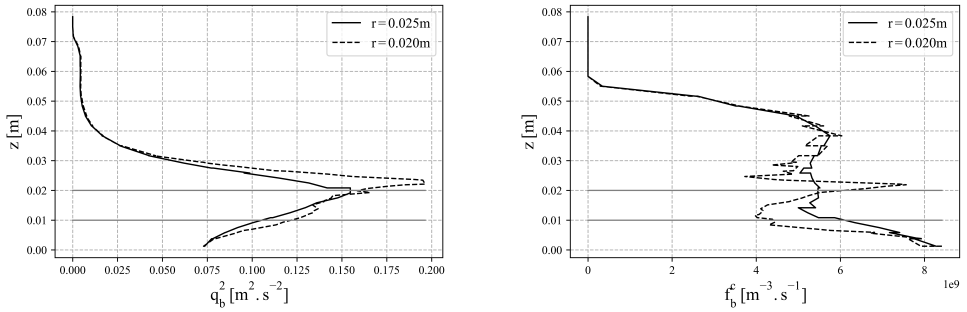

(a) (b)

FIG. 7: z - profile of (a) bead kinetic energy and (b) bead collision frequency.

the propeller. Particles break more under the propeller and close to the wall. Hence, the mean diameter of particles is smaller at this place.

6. CONCLUSION

Based upon theoretical analyses, breakage kernel has been modeled. This function depends on local values. Breakage efficiency depends on three simultaneous conditions. First, by assuming that the milling is achieved by the collision between two grinding beads, the collision frequency has to be high. The second one implies the presence of the powder between the two colliding beads. The third one concerns the available energy of the beads which must be high enough to break the powder particles.

Two coupled methods to track the particle size distribution evolution have been presented. Preliminary numerical simulation results of the one particle granular flow method are given in the last part of the article. Those results have shown, on one hand that hydrodynamics is highly heterogeneous and should be considered for modeling wet miling: the standard hypothesis of a perfectly mixed milling process (Nomura et al., 1991a; Oliveira et al., 2020) omits key physical

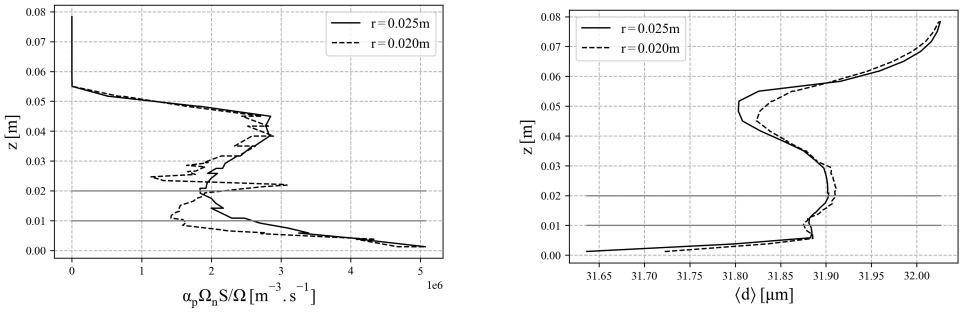

(a) (b)

FIG. 8: z - profile of (a) particle break frequency and (b) mean diameter.

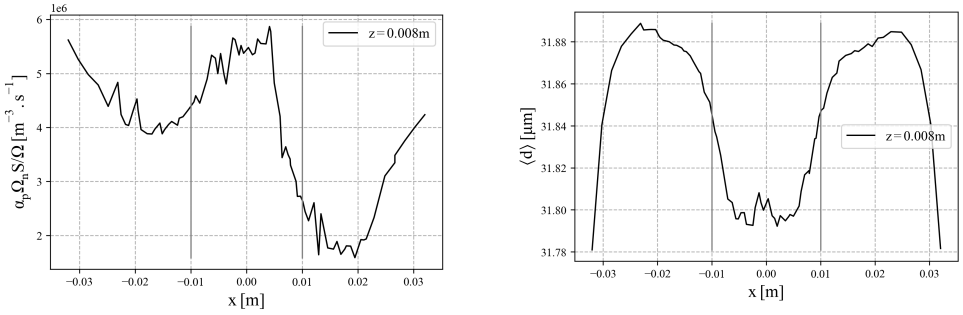

(a) (b)

FIG. 9: x - profile of (a) particle break frequency and (b) mean diameter.

aspects of the breakage process and thus cannot be predictive about the process performances.. On the other hand, those results give us an overview of the quantity that one should consider to evaluate the efficiency of the milling process.

As a prospect, both of the coupling methods should be compared, to quantify the variation of results when the assumption of one particle granular flow is done. Experimental investigations have to be carried out, to validate the models used for breakage kernel.

ACKNOWLEDGMENTS

The authors would like to acknowledge the financial support of Orano and EDF.

REFERENCES

Beinert, S., Schilde, C., Gronau, G., and Kwade, A., Cfd-discrete element method simulations combined with compression experiments to characterize stirred-media mills, *Chemical Engineering & Technology*, vol. **37**, no. 5, pp. 770–778, 2014.

Bennani, L., Neau, H., Baudry, C., Laviéville, J., Fede, P., and Simonin, O., Numerical simulation of unsteady dense granular flows with rotating geometries, *Chemical Engineering Research and Design*, vol. **120**, pp. 333–347, 2017.

Bilgili, E. and Guner, G., Mechanistic modeling of wet stirred media milling for production of drug nanosuspensions, *AAPS PharmSciTech*, vol. **22**, no. 1, pp. 1–23, 2021.

Bilgili, E. and Scarlett, B., Population balance modeling of non-linear effects in milling processes, *Powder Technology*, vol. **153**, no. 1, pp. 59–71, 2005.

Capece, M., Bilgili, E., and Dave, R., Identification of the breakage rate and distribution parameters in a non-linear population balance model for batch milling, *Powder technology*, vol. **208**, no. 1, pp. 195–204, 2011.

Deglon, D.A. and Meyer, C.J., Cfd modelling of stirred tanks: Numerical considerations, *Minerals Engineering*, vol. **19**, no. 10, pp. 1059–1068, 2006.

Fede, P., Simonin, O., and Ingram, A., 3d numerical simulation of a lab-scale pressurized dense fluidized bed focussing on the effect of the particle-particle restitution coefficient and particle–wall boundary conditions, *Chemical Engineering Science*, vol. **142**, pp. 215–235, 2016.

Fede, P., Simonin, O., and Villedieu, P., Monte-carlo simulation of colliding particles or coalescing droplets transported by a turbulent flow in the framework of a joint fluid–particle pdf approach, *International Journal of Multiphase Flow*, vol. **74**, no. 0, pp. 165 – 183, 2015.

Gers, R., Anne-Archard, D., Climent, E., Legendre, D., and Frances, C., Two colliding grinding beads: Experimental flow fields and particle capture efficiency, *Chemical engineering & technology*, vol. **33**, no. 9, pp. 1438–1446, 2010.

Kumar, J., Peglow, M., Warnecke, G., and Heinrich, S., An efficient numerical technique for solving population balance equation involving aggregation, breakage, growth and nucleation, *Powder Technology*, vol. **182**, no. 1, pp. 81–104, 2008.

Kumar, S. and Ramkrishna, D., On the solution of population balance equations by discretization—i. a fixed pivot technique, *Chemical Engineering Science*, vol. **51**, no. 8, pp. 1311–1332, 1996.

Kwade, A., Determination of the most important grinding mechanism in stirred media mills by calculating stress intensity and stress number, *Powder Technology*, vol. **105**, no. 1-3, pp. 382–388, 1999a.

Kwade, A., Determination of the most important grinding mechanism in stirred media mills by calculating stress intensity and stress number, *Powder Technology*, vol. **105**, no. 1-3, pp. 382–388, 1999b.

Laviéville, J., Simonin, O., Berlemont, A., and Chang, Z., Validation of inter-particle collision models based on Large Eddy Simulation in gas-solid turbulent homogeneous shear flow, *Proc. 7th Int. Symp. on Gas-Particle Flows ASME FEDSM97-3623.*, pp. –, 1997.

Lun, C. and Savage, S., The effects of an impact velocity dependent coefficient of restitution on stresses developed by sheared granular materials, *Acta Mechanica*, vol. **63**, no. 1, pp. 15–44, 1986.

Neau, H., Pigou, M., Fede, P., Ansart, R., Baudry, C., Mérigoux, N., Laviéville, J., Fournier, Y., Renon, N., and Simonin, O., Massively parallel numerical simulation using up to 36,000 cpu cores of an industrial-scale polydispersed reactive pressurized fluidized bed with a mesh of one billion cells, *Powder Technology*, vol. **366**, pp. 906–924, 2020.

Nomura, S., Hosoda, K., and Tanaka, T., An analysis of the selection function for mills using balls as grinding media, *Powder technology*, vol. **68**, no. 1, pp. 1–12, 1991a.

Nomura, S., Hosoda, K., and Tanaka, T., An analysis of the selection function for mills using balls as grinding media, *Powder technology*, vol. **68**, no. 1, pp. 1–12, 1991b.

Oliveira, A., Rodriguez, V., De Carvalho, R., Powell, M., and Tavares, L., Mechanistic modeling and simulation of a batch vertical stirred mill, *Minerals Engineering*, vol. **156**, p. 106487, 2020.

Roustan, M., Pharamond, J.C., and Line, A., *Agitation. Melange: Concepts Theoriques Base*, Ed. Techniques Ingénieur, 1999.

Saffman, P. and Turner, J., On the collision of drops in turbulent clouds, *Journal of Fluid Mechanics*, vol. **1**, no. 1, pp. 16–30, 1956.

Shiea, M., Buffo, A., Vanni, M., and Marchisio, D., Numerical methods for the solution of population balance equations coupled with computational fluid dynamics, *Annual review of chemical and biomolecular*

engineering, vol. **11**, pp. 339–366, 2020.